

PROCEEDINGS OF THE XIX ALL-RUSSIAN CONFERENCE
ON PHYSICS OF FERROELECTRICS (VKS-XIX)

(Moscow, Russia, June 19–23, 2011)

**XAFS Studies of the Local Structure and Charge State
of the Pr Impurity in SrTiO₃**

I. A. Sluchinskaya^{a,*}, A. I. Lebedev^a, and A. Erko^b

^a *Moscow State University, Moscow, 119991 Russia*

* *e-mail: irinasluch@nm.ru*

^b *Berliner Elektronenspeicherring-Gesellschaft für Synchrotronstrahlung (BESSY),
Albert-Einstein-Str. 15, Berlin, 12489 Germany*

Abstract—Solid solutions of (Sr_{1-x}Pr_x)TiO₃ have been studied using X-ray methods. It has been shown that, with an increase in the praseodymium concentration, the temperature of the structural phase transition to the phase with space group *I4/mcm* increases and, at $x \geq 0.15$, the structure at 300 K is tetragonal. X-ray absorption fine structure (XAFS) spectroscopy studies have revealed that Pr ions are predominantly in the charge state 3+ and occupy the Sr sites. No indications of the off-centering of Pr atoms at the Sr sites have been revealed. The local environment of Pr atoms is characterized by a strong relaxation of the oxygen atoms, the value of which corresponds to the difference between the ionic radii of Pr³⁺ and Sr²⁺. It has been found that, in the second shell, there occurs a significant repulsion of the Pr³⁺ and Ti⁴⁺ ions, which is responsible for the weak dependence of the lattice parameter in the solid solution on the praseodymium concentration.

DOI: 10.1134/S1063783412050381

1. INTRODUCTION

Strontium titanate SrTiO₃ is an incipient ferroelectric with a cubic structure at 300 K, in which quantum fluctuations stabilize the paraelectric phase down to very low temperatures. At temperatures close to 105 K, it undergoes a structural phase transition to the tetragonal phase with space group *I4/mcm* due to rotations of the octahedra. The ferroelectric state in SrTiO₃ can be induced either by applying external electric or strain fields or by doping this compound with impurities. In this case, the temperature of the phase transition, as a rule, remains relatively low [1].

In this respect, the results recently obtained by Durán et al. [2] for SrTiO₃ samples doped with the praseodymium impurity appeared to be interesting and unexpected. It was found that these samples exhibit a maximum of the dielectric constant at approximately 240°C and hysteresis loops at room temperature [2], which were explained by the ferroelectric phase transition occurring in the crystals. A specific feature of this phase transition was a weak influence of the Pr concentration on the temperature corresponding to the maximum of the dielectric constant, which differed from the influence exerted by other impurities on the ferroelectric phase transition in SrTiO₃ [1]. An analysis of the X-ray photoelectron spectra enabled the authors of [2] to draw the conclusion that the Pr atoms in SrTiO₃ are in two charge

states (3+ and 4+). Synchrotron X-ray diffraction studies [3] revealed a tetragonal lattice distortion in (Sr_{0.85}Pr_{0.15})TiO₃ whose structure was determined as *P4mm*. Further investigations [4–6] carried out using X-ray powder diffraction, neutron diffraction, and Raman spectroscopy demonstrated that, with an increase in the Pr concentration, the temperature of the structural phase transition to the *I4/mcm* phase rapidly increases and, at the praseodymium concentration $x = 0.05$, is close to 300 K. The temperature dependence of the frequency of soft TO phonons in (Sr_{0.975}Pr_{0.025})TiO₃ crystals did not reveal specific features at the temperature of the dielectric anomaly [4]; therefore, the conclusion was drawn that no ferroelectric phase transition occurs in the SrTiO₃ matrix. The observation of the dispersion of the dielectric constant [4] showed that the system demonstrates signs of a high-temperature relaxor ferroelectric and that the temperature of the transition to the ferroelectric state is not related to the temperature of the structural phase transition. In order to explain the observed anomalies in the dielectric constant, the following models were proposed in [2–6]: (1) the displacive phase transition, (2) the distortion of TiO₆ octahedra due to the replacement of strontium atoms by praseodymium atoms, and (3) the formation of polar nanoregions either as a result of the formation of “defect states” or as a result of the off-centering of Pr atoms.

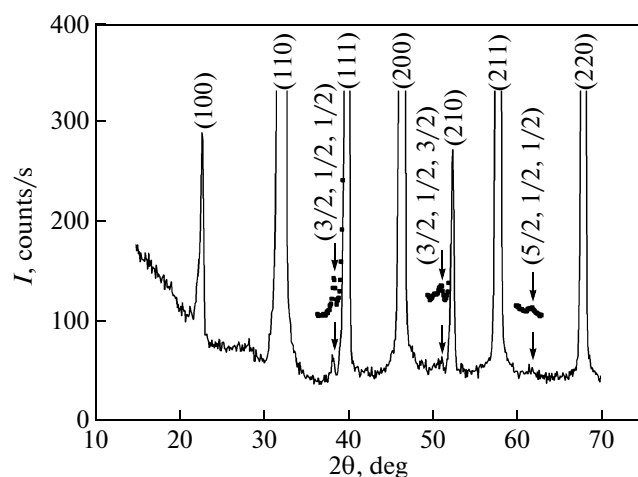


Fig. 1. X-ray diffraction pattern of the $(\text{Sr}_{0.85}\text{Pr}_{0.15})\text{TiO}_3$ sample annealed at 1400°C . Points represent fragments of the X-ray diffraction pattern that are shifted along the vertical axis and recorded for an accumulation time of 300 s. Arrows indicate the calculated positions of the superstructure reflections.

Another reason for the interest expressed by researchers in $\text{SrTiO}_3(\text{Pr})$ solid solutions is that the Pr impurity atoms have magnetic moments, which makes possible the appearance of magnetic ordering and properties characteristic of multiferroics in the samples.

X-ray absorption fine structure (XAFS) spectroscopy studies of the local structure and charge state of the Pr impurity in SrTiO_3 are important because of the contradictory data on the crystal structure, the location of Pr atoms, and their charge state, as well as because of the lack of reliable data on the microscopic structure and mechanisms providing electroneutrality upon the heterovalent substitution.

2. SAMPLE PREPARATION AND EXPERIMENTAL TECHNIQUE

Samples of the nominal composition $(\text{Sr}_{1-x}\text{Pr}_x)\text{TiO}_3$ with $x = 0.05\text{--}0.30$, and $\text{Sr}(\text{Ti}_{1-x}\text{Pr}_x)\text{O}_3$ with $x = 0.05$ were prepared by the solid-phase reaction method. The initial components were as follows: SrCO_3 , nanocrystalline TiO_2 synthesized by the hydrolysis of tetrapropylorthotitanate and dried at 500°C , and Pr_6O_{11} . The components were weighed in the required proportions, ground under acetone until the mixture was completely dried, and annealed in air at 1100°C for 8 h. The obtained powders were ground once again and additionally annealed at temperatures in the range from 1100 to 1600°C . The annealing times were as follows: 8 h at 1100°C , 4 h at 1300 and 1400°C , and 2 h at 1600°C . In the samples annealed at 1100°C , praseodymium had not yet entered into the reaction; solid solutions were formed beginning from 1300°C .

Extended X-ray absorption fine structure (EXAFS) and X-ray absorption near-edge structure (XANES) spectra were recorded by detecting X-ray fluorescence with a RÖNTEC energy dispersive detector. The investigations were performed at the BESSY synchrotron radiation source on the KMC-2 station at the Pr L_{II} absorption edge (6.440 keV) and the Ti K absorption edge (4.966 keV) at 300 K. The choice of the L_{II} edge, instead of the L_{III} edge, was motivated by the fact that the Pr L_{α_1} fluorescence line excited at the L_{III} edge almost completely coincides with the Ti K_{β_1} fluorescence line, which significantly complicates the detection of the signal from Pr atoms. For the chosen Pr L_{II} edge, the L_{β_1} fluorescence line is excited and separated by 560 eV from the Ti fluorescence line. The EXAFS spectra were processed using the conventional method [7].

3. RESULTS AND DISCUSSION

The X-ray diffraction analysis has revealed that the $\text{Sr}(\text{Ti}_{1-x}\text{Pr}_x)\text{O}_3$ ($x = 0.05$) samples synthesized at annealing temperatures in the range from 1300 to 1600°C are two-phase and, as can be judged from additional lines in the X-ray diffraction pattern, contain the Ruddlesden–Popper phases $\text{Sr}_3\text{Ti}_2\text{O}_7$ and Pr_6O_{11} ; the $(\text{Sr}_{1-x}\text{Pr}_x)\text{TiO}_3$ ($x = 0.05\text{--}0.15$) samples are single-phase; and the sample with $x = 0.3$ contains a small amount of the second phase $\text{PrO}_{2-\delta}$.

The X-ray diffraction patterns of the $(\text{Sr}_{1-x}\text{Pr}_x)\text{TiO}_3$ samples with $x = 0.15\text{--}0.30$, along with the reflections characteristic of the cubic perovskite phase, exhibit additional superstructure reflections whose intensity increases with an increase in the Pr concentration. The superstructure reflections indicated by arrows in Fig. 1 can be indexed in terms of the cubic lattice as the lines with the $(3/2, 1/2, 1/2)$, $(3/2, 1/2, 3/2)$, and $(5/2, 1/2, 1/2)$ indices. In accordance with the results reported in the paper by Glazer [8], the appearance of these reflections suggests that the oxygen octahedra are rotated around the c axis according to the scheme $a^0a^0c^-$; in this case, the symmetry of the crystal lattice is reduced from cubic to tetragonal (space group $I4/mcm$). Since the structural phase transition in undoped SrTiO_3 occurs at 105 K, it can be concluded that, at $x \geq 0.15$, the temperature of this phase transition exceeds 300 K. Our conclusions agree with the conclusions drawn from the neutron diffraction studies [6]; however, it should be noted that, in our work, the complete set of superstructure reflections was observed using X-ray diffraction for the first time. An increase in the temperature of the structural phase transition upon doping with praseodymium is not surprising, because the ionic radius of praseodymium is considerably smaller than the ionic radius of strontium.

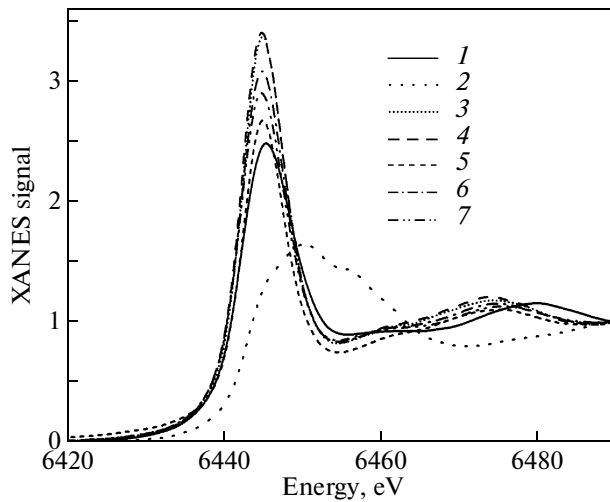


Fig. 2. Pr L_{II} XANES spectra of the $\text{SrTiO}_3(\text{Pr})$ samples and reference compounds of trivalent and tetravalent praseodymium: (1) $\text{Pr}_2\text{Ti}_2\text{O}_7$; (2) BaPrO_3 ; (3–5) $(\text{Sr}_{0.95}\text{Pr}_{0.05})\text{TiO}_3$ samples annealed at 1300, 1400, and 1600°C, respectively; (6) $(\text{Sr}_{0.85}\text{Pr}_{0.15})\text{TiO}_3$ annealed at 1400°C; and (7) $(\text{Sr}_{0.7}\text{Pr}_{0.3})\text{TiO}_3$ sample annealed at 1400°C. The spectra were recorded at 300 K.

The parameters of pseudocubic lattice¹ for the $(\text{Sr}_{1-x}\text{Pr}_x)\text{TiO}_3$ samples annealed at 1400°C are as follows: $a = 3.897 \text{ \AA}$ for $x = 0.05$, $a = 3.898 \text{ \AA}$ for $x = 0.15$, and $a = 3.894 \text{ \AA}$ for $x = 0.30$. It is seen that the lattice parameter decreases only slightly with an increase in the Pr concentration. According to the data reported in [2, 5, 6], the lattice parameter of the $(\text{Sr}_{1-x}\text{Pr}_x)\text{TiO}_3$ compounds after doping remains almost unchanged.

In order to determine the charge state of the Pr impurity, the XANES spectra of the samples under investigation were compared with those of the reference compounds. The XANES spectra for five samples of the $(\text{Sr}_{1-x}\text{Pr}_x)\text{TiO}_3$ solid solutions and reference compounds BaPrO_3 and $\text{Pr}_2\text{Ti}_2\text{O}_7$ are shown in Fig. 2. From a comparison of these spectra, it can be concluded that, irrespective of the praseodymium concentration and the preparation conditions, the Pr ions are predominantly in the charge state 3+.

The structural positions of the impurity ions were determined by analyzing the EXAFS spectra. The characteristic spectrum of the extended X-ray absorption fine structure χ as a function of the photoelectron wave vector k for the $(\text{Sr}_{0.85}\text{Pr}_{0.15})\text{TiO}_3$ sample and its best theoretical approximation are shown in Fig. 3. The best agreement between the calculated and experimental spectra is achieved in the model in which strontium atoms are replaced by praseodymium

¹ The lattice parameters a and c in the tetragonal phase are so close to each other that, in our experiments, they could not be measured independently. Therefore, the lattice of our samples is considered to be pseudocubic.

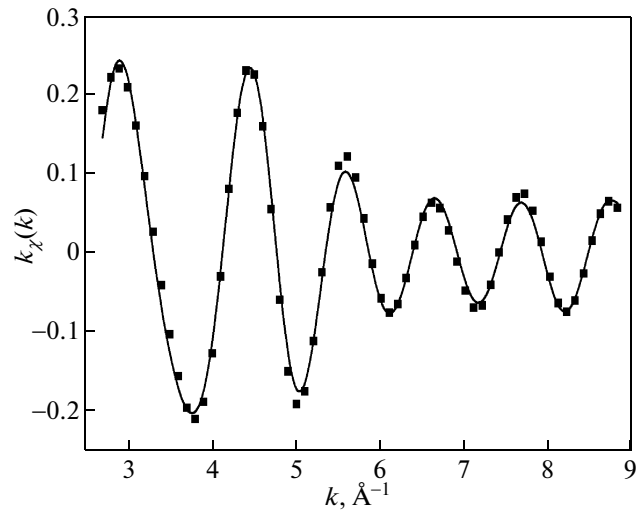


Fig. 3. Pr L_{II} EXAFS spectrum of the $(\text{Sr}_{0.85}\text{Pr}_{0.15})\text{TiO}_3$ sample annealed at 1400°C. Points are experimental data, and the solid line shows their best theoretical approximation. The spectrum was recorded at 300 K.

atoms. The interatomic distances and Debye–Waller factors for the three nearest shells are presented in the table. A comparison of the obtained distances with the average interatomic distances calculated from the measured lattice parameter has demonstrated that strong relaxations around the impurity atom manifest themselves only in the first shell ($\Delta R \approx -0.136 \text{ \AA}$). In the second shell, by contrast, there is a slight increase in the average interatomic distance ($\Delta R \approx +0.02 \text{ \AA}$). The accuracy in determining the parameters of the third shell is insufficient to draw any conclusions, but the distance to this shell is in agreement with the X-ray diffraction data.

The relatively low values of the Debye–Waller factors for the second shell, which correspond to typical values of the amplitude of thermal vibrations at 300 K in perovskites, allow us to exclude almost completely the possibility of manifesting the off-centering of Pr atoms. The unexpectedly high Debye–Waller factor for the first shell in the sample with $x = 0.15$ is explained by the rotations of the octahedra revealed from the X-ray measurements, when the lengths of twelve Pr–O bonds become different. In the sample with $x = 0.05$, the high value of the Debye–Waller factor can indicate a large amplitude of thermal rotations of the octahedra, because, according to [5], the temperature of the structural phase transition at this praseodymium concentration is close to room temperature.

The possibility of incorporating Pr atoms into the B sites of the perovskite structure was verified by comparing the experimental EXAFS spectra with the calculated spectra obtained in the model allowing for the simultaneous incorporation of the impurity atoms into the A and B sites. With an increase in the fraction of the

Structural parameters obtained from the processing of the EXAFS spectra (R_i is the distance to the i th shell, and σ_i^2 is the Debye–Waller factor for this shell)

| Sample | Shell | R_i , Å | σ_i^2 , Å ² |
|---|-------|-----------|-------------------------------|
| (Sr _{0.95} Pr _{0.05})TiO ₃ , annealing at 1300°C | Pr–O | 2.629(9) | 0.017(1) |
| | Pr–Ti | 3.394(5) | 0.003(1) |
| | Pr–Sr | 3.887(34) | 0.022(5) |
| (Sr _{0.95} Pr _{0.05})TiO ₃ , annealing at 1600°C | Pr–O | 2.623(7) | 0.014(1) |
| | Pr–Ti | 3.388(4) | 0.003(1) |
| | Pr–Sr | 3.926(13) | 0.012(2) |
| (Sr _{0.85} Pr _{0.15})TiO ₃ , annealing at 1400°C | Pr–O | 2.608(15) | 0.020(2) |
| | Pr–Ti | 3.404(8) | 0.004(1) |
| | Pr–Sr | 3.930(38) | 0.018(5) |
| (Sr _{0.95} Pr _{0.05})TiO ₃ , ($a = 3.897$ Å) | Sr–O | 2.756 | |
| | Sr–Ti | 3.375 | |
| | Sr–Sr | 3.897 | |

impurity atoms in the B sites, the agreement between the experimental and calculated curves becomes worse. This means that the probability of the incorporation of impurity atoms into the B sites is relatively low, which, most likely, is associated with a very strong difference between the ionic radii of Ti⁴⁺ (0.605 Å) and Pr³⁺ (0.990 Å) in the octahedral coordination [9].

In this work, it was established that the Pr³⁺ ions are located in the A sites of the perovskite structure and are on-center; therefore, their charge state 3+ suggests the appearance of vacancies in order to ensure the electroneutrality. These vacancies can be both V_{Sr} and V_O . The possibility of reducing titanium to the Ti³⁺ state can be excluded, because, otherwise, the samples would acquire a dark color. The investigation of the pre-edge structure at the Ti K absorption edge for the (Sr_{0.95}Pr_{0.05})TiO₃ sample did not reveal an increase in the intensity of the transition $1s \rightarrow 3d(e_g)$, which is forbidden in the dipole approximation [10]. This indicates that oxygen vacancies in the octahedra are almost completely absent. On the other hand, if the electroneutrality would be provided by the formation of V_{Sr} , the excess of Sr atoms in the sample should lead to the formation of Ruddlesden–Popper phases at approximately the same intensity as in the case of Sr(Ti_{0.95}Pr_{0.05})O₃. The X-ray diffraction patterns did not exhibit any indications of these phases; however, this can be associated with very small sizes of the corresponding precipitates.

The observed decrease in the interatomic distance in the first shell is completely consistent with the difference between the ionic radii of Pr³⁺ and Sr²⁺.

Because there are no data for the Pr³⁺ ion in the twelvefold coordination, we used the data obtained for the eightfold coordination: $R_{Sr} = 1.26$ Å and $R_{Pr} = 1.126$ Å [9]. The difference between the ionic radii of these ions is equal to 0.134 Å, which coincides with the value found in our study for the relaxation (−0.136 Å). At the same time, our distances to the second shell turned out to be even slightly overestimated. In our opinion, this can be explained by the fact that the charge of the Pr impurity ion exceeds the charge of the Sr ion, which enhances the repulsion between the Pr³⁺ and Ti⁴⁺ ions and increases the Pr–Ti distance. The fact that we did not reveal significant incorporation of praseodymium atoms into the B sites of the perovskite structure makes impossible the explanation of the constancy of the lattice parameter by partial substitution of the B sites [5]. In our opinion, the weak dependence of the lattice parameter on the praseodymium concentration is explained by the repulsion between the Pr and Ti atoms.

Although, in this paper, we concerned only the structural aspects of SrTiO₃(Pr), nonetheless, we found that praseodymium is not an off-center impurity and does not cause a significant distortion of the TiO₆ octahedra. The model of ferroelectricity in the system of frozen electric dipoles, in our opinion, is also untenable; therefore, none of the models listed in the Introduction can explain the appearance of the dielectric anomalies. The absence of an influence of the Pr impurity on the soft mode [4] suggests that the observed dielectric anomalies are not related to the bulk of the crystal. In our opinion, the possible cause of their occurrence can be the emergence of electrical conductivity due to hopping of electrons between Pr atoms, which can exist in two charge states (Pr³⁺ and Pr⁴⁺). Even at a very low concentration of Pr⁴⁺ centers, because of the large distances over which electrons are transferred, the changes in dipole moments can be large enough, thus leading to significant observable effects.

ACKNOWLEDGMENTS

The authors are grateful to V.F. Kozlovskii for his assistance in performing the X-ray measurements.

REFERENCES

1. V. V. Lemanov, *Ferroelectrics* **226**, 133 (1999).
2. A. Durán, E. Martínez, J. A. Díaz, and J. M. Siqueiros, *J. Appl. Phys.* **97** (10), 104109 (2005).
3. A. Durán, F. Morales, L. Fuentes, and J. M. Siqueiros, *J. Phys.: Condens. Matter* **20** (8), 085219 (2008).

4. R. Ranjan, R. Hackl, A. Chandra, E. Schmidbauer, D. Trots, and H. Boysen, *Phys. Rev. B: Condens. Matter* **76** (22), 224109 (2007).
5. R. Ranjan, R. Garg, R. Hackl, A. Senyshyn, E. Schmidbauer, D. Trots, and H. Boysen, *Phys. Rev. B: Condens. Matter* **78** (9), 092102 (2008).
6. R. Garg, A. Senyshyn, H. Boysen, and R. Ranjan, *Phys. Rev. B: Condens. Matter* **79** (14), 144122 (2009).
7. A. I. Lebedev, I. A. Sluchinskaya, V. N. Demin, and I. Manro, *Izv. Akad. Nauk, Ser. Fiz.* **60** (10), 46 (1996).
8. A. M. Glazer, *Acta Crystallogr., Sect. A: Cryst. Phys., Diffraction, Theor. Gen. Crystallogr.* **31**, 756 (1975).
9. R. D. Shannon, *Acta Crystallogr., Sect. A: Cryst. Phys., Diffraction, Theor. Gen. Crystallogr.* **32**, 751 (1976); <http://abulafia.mt.ic.ac.uk/shannon/>
10. A. I. Lebedev, I. A. Sluchinskaya, A. Erko, A. A. Veligzhanin, and A. A. Chernyshov, *Phys. Solid State* **51** (5), 991 (2009).

Translated by O. Borovik-Romanova